J. Indian Inst. Sci.
A Multidisciplinary Reviews Journal
ISSN: 0970-4140 Coden-JIISAD

REVIEW ARTICLE

Recent Advancements in 3-D Structure Determination of Bacteriophages: from Negative Stain to CryoEM

*Sayani Das and Amar N. Ghosh**

Abstract | For many years, X-ray crystallography has been exclusively used by structural biologists for resolving virus structures and viral proteins at atomic resolution level. However, the discovery of electron microscopy, especially Cryo-electron microscopy (cryoEM), has enabled us to visualise the detailed structural features of biological macromolecules in a more accurate way. In recent years, cryoEM has made sudden progress in its use due to high-end microscopes, improved detectors and modernised software. It is now possible to get near-atomic resolution three-dimensional viral maps using cryoEM. Among viruses, the bacterial viruses or bacteriophages are the most fascinating objects for the structural biologists as they are highly symmetrical particles. The development of cryoEM has also made it easy to determine the structures of these highly symmetrical macromolecules at near-atomic resolution.

Keywords: *Bacteriophage, Electron microscopy, CryoEM, Negative stain*

1 Introduction

Bacterial viruses or bacteriophages were first reported by the British bacteriologist Twort.[1] He found an infectious agent in a culture of staphylococcus which can change the colonial morphology of the bacterium. In 1917 Felix d'Herelle published a brief note describing a new kind of microbe which is now regarded as a bacteriophage.[1, 2] Since then, a vast amount of research is being done on possible therapeutic applications of bacteriophages.[1, 3, 4]

Apart from its use in therapeutics, phages are also used in various typing schemes of different bacteria and in studying the spread of epidemics. With five vibriophages, a typing scheme for *V. cholerae* bacteria was described by Chakrabarti et al.[5] Bacteriophages are the smallest known biological systems, therefore, they are widely used as model systems for studying biological processes at the macromolecular level. Besides, they have been used in host genetic studies. However, structural information, especially the three-dimensional structure of bacteriophages, is predominantly needed for predicting their uses.

The discovery of electron microscope had opened a vast area of research on viruses and bacteriophages. Later, the development of cryo-electron microscopy (cryoEM) has enriched the field of structural biology by allowing biological samples to be visualized under electron microscope in frozen-hydrated, unstained condition. Though many groups have tried to study frozen, unstained specimens[6, 7], Dubochet and his colleagues were the first who successfully produced images of frozen-hydrated, unstained bacteriophage T4 in 1983.[8] During the last 10 years, the advancement in every aspect of cryoEM has made it possible to obtain three-dimensional structures of various biological samples at near-atomic resolution.

Viruses, especially bacteriophages, being highly symmetric large molecular masses have played pivotal role as a model system for further development of imaging techniques and three-dimensional reconstruction processes following electron microscopy. CryoEM requires a good deal of image processing as the contrast of unstained sample is very low. Image processing

Phage typing: it is a method used for differentiating bacterial strains and tracing the source of outbreaks of bacterial infection.

[1] *Division of Electron Microscopy, ICMR-National Institute of Cholera and Enteric diseases, P-33, C.I.T Road, Scheme-XM, Beleghata, Kolkata 700010, India.*
**ghosh.an@icmr.gov.in*

from EM data had started much earlier than obtaining frozen-hydrated image of samples. The tail structure of bacteriophage T4 was first three-dimensionally reconstructed from 2-D EM images in 1968.[9] Icosahedral viral capsids because of their highly symmetric structure and abundant availability are often studied by single-particle cryoEM. In recent years, the improvement in structure determination of phages from nanometre to near-atomic resolution is very much fascinating, as it allows visualization of phage structures in details. Nowadays, near-atomic resolution structure of a wide range of virus particles is available in the literature.

High-resolution three-dimensional structures of phages are being used to form the atomic model for showing arrangements of protein subunits. These atomic models are useful for predicting viral assembly and maturation. The icosahedral virus structures at near-atomic resolution can also reveal the structure of genome present inside of it.[10] Due to advancement in every aspect of cryoEM as well as image reconstruction softwares, it has been possible to obtain the structure of mutant T4 phage capsid at near-atomic resolution of 3.3 Å.[11] In very near future, viral structures below 3 Å resolution are expected to be determined routinely.

Negative staining: in this staining method, the background is stained, without staining the actual specimen. Due to contrast with the background, the specimen is visible.

2 Background

The first known virus structure was of tobacco mosaic virus (TMV) by Stanley's work and X-ray diffraction studies by Bernal and Fankuchen in the 1930s.[12] During that time it became evident that crystals of small RNA plant and animal viruses could diffract X-rays, suggesting viruses have distinct structural features. Further, the discovery of DNA structure in 1953 led Crick and Watson[12] to suggest that viral genome possess many identical copies of viral capsid protein. Therefore, they suggested that the capsid of spherical viruses might have the symmetry of regular polyhedral and this prediction was verified by Caspar,[13] who showed that tomato bushy stunt virus (TBSV) has icosahedral symmetry. Though many small plant viruses were crystallized by X-ray diffraction studies (tomato bushy stunt virus,[13] yellow mosaic virus[14]), it was difficult to crystallize big animal or bacterial viruses due to their heterogeneous structure. Some of the issues in studying crystalline viruses were to resolve the individual Bragg reflections because of the large unit cell sizes, measuring the intensities of many reflections by visual inspection of the black spots on a film, recording all data by hand without any electronic computers and lack of ways to solve the crystallographic phase problem.[12]

Single-particle method: it is a group of computerized image processing techniques, which use multiple images of the same particle taken by TEM.

Icosahedral symmetry: a regular icosahedron has 60 rotational symmetries.

After the discovery of electron microscope in 1931 by Max Knoll and Ernst Ruska, in 1942 Helmut Ruska, brother of Ernst Ruska, first showed the pictures of bacteriophage of *E. coli* bacterium taken with the 'hypermicroscope'.[15] Later, metal shadow casting was introduced to observe viruses with greater contrast by William.[16] Shadow casting method gave us the information about the size and shape of viruses without revealing their internal structure. It also enhanced the roughness of the substrate–film which made detail observation of small viruses difficult. In 1959, Brenner and Horne introduced "negative staining" method which involves mixing of virus samples in aqueous medium with 1% phosphotungstic acid and spraying the mixture directly onto electron microscope supporting films.[17] The technique was first applied to tobacco mosaic virus and turnip yellow mosaic virus. This technique immensely enhanced the contrast and resolvability of the virus particles.

In 1968, De Rosier and Klug applied Fourier transformation method which estimated the symmetry of T4 phage tail and had reconstructed three-dimensional structure of the tail.[9] However, in 1971 R. A. Crowther described the process of determining three-dimensional structure of a virus particle from negatively stained images through computational approach.[18] The paper describes how the images of symmetric virus particles in different orientations from electron micrographs were used to determine three-dimensional structure by the process commonly called nowadays as 'single particle analysis' method.[19] Although, some of the viruses like HIV, influenza virus and many others have variations in their structures, they cannot be easily reconstructed by single-particle analysis method due to their variability. Therefore, to reconstruct them cryoET (cryo-electron tomography) is the method of choice.[20, 21] In this procedure, the stage is tilted in different orientations to give different projections of sample that are combined to form a three-dimensional image. However, radiation damage limits the time of exposure for each projection leading to formation of low-resolution structures. CryoET is also the method of choice to study phage–host interaction.

Irrespective of different reconstruction techniques, three-dimensional reconstructions from negatively stained images were hampered due to uneven staining and stain distortions of the sample. Furthermore, the reconstructed map showed

only the stained structural features leading to formation of two-dimensional reconstructed image with low resolution. This situation was drastically changed when in early 1980s, Dubochet and his colleagues introduced the concept of cryoEM by freezing samples in liquid nitrogen or ethane, thereby avoiding stain distortions and observing unfixed, unstained samples free from the kind of damage caused by dehydration, freezing or adsorption to a support.[8] Since then, cryo-fixed samples are being routinely used for three-dimensional structure determination of viruses and have now become a powerful rival of X-ray crystallography.[22]–[24] Also, cryoEM has the added advantage of phase image over x-ray crystallography. In 2017, Jacques Dubochet, Joachim Frank and Richard Henderson were awarded the prestigious Nobel Prize in chemistry for developing cryo-electron microscopic techniques for high-resolution structure determination of macromolecules.

3 Preference for Cryo-electron Microscopy over X-ray Crystallography for Viral Structure Determination

X-ray crystallography was the only choice to the structural virologists for determining the viral structures by making crystals.[25, 26] So far many viral structures have been solved by crystallography. However, it is difficult to crystallize the large virus structures as they are often formed with heterogeneous protein subunits. In contrast, cryoEM can easily be used to obtain authentic virion structures in a short span of time making it preferable method of choice for structural biologists.[27] Among the cryoEM subfields, single-particle 3-D reconstruction of icosahedral viruses has been used for achieving near-atomic resolutions (3–4 Å) and is now considered a preferred approach over X-ray crystallography.[22]

Determination of detailed structural information of a virus through cryoEM depends on the resolution.[28] As resolution increases, there is more possibility to extract detailed information from the density map. Low-resolution (20–10 Å) maps can be used to identify general features like viral morphology, shape and sizes. However, high-resolution density map usually at sub-nanometer resolutions (9–6 Å) allows identification of individual subunit boundaries and secondary structure elements (SSEs).[29] At this resolution, α-helices and β-sheets can be visualized as long rod-like densities and as thin continuous planes, respectively. When the resolution reaches approximately 4.5 Å or better, a complete atomic model can be formed.[29] In addition, beyond 4.5 Å resolution, individual pitch of α-helices and separate strands of β-sheet become evident.[30]

Both instrumentation and image processing developments are critical in the evolution of structural biology in 3D-EM field. An example of the success of cryoEM methodology was the development of cold stages that allowed imaging of samples at liquid nitrogen temperature without lowering the resolution. Advancement in microscope technology such as field emission gun (FEG), intermediate voltages or improved illumination systems, and automation of data collection have also improved the image quality.[31] Furthermore, in some cryoEM data collection session, a percentage of micrographs were often discarded due to beam-induced motion, a phenomenon known as "blurring" of the image.[32] Recently, powerful new image processing algorithms have been developed for the correction of beam-induced motion and the classification of distinct structural states. Another major shortcoming has been the poor performance of digital cameras, especially at the preferred electron energy for imaging biological samples (300 keV). Hence, during the last few years the cryoEM field has undergone what some are now describing as a "revolution".[33] This positive transformation relates to the advent of the first commercial direct electron detection devices (DDDs) after years of development at the MRC-LMB by Henderson and Faruqui, and at LBNL and UCSD by Denes et al.[34] The higher signal-to-noise ratio of these detectors with respect to traditional film or the scintillator-based CCD cameras, is an obvious gain in a field limited by low signal. Also the fast read out of the DDD allowed splitting the total dose into short frames where the blurring due to beam-induced movement is minimized, and where frame alignment is carried out computationally after data collection.[35]–[37]

4 Evolution of Imaging Practices in Virus Research

After its discovery in 1959 by Brenner and Horne,[17] negative-staining method is widely employed on viruses for structure determination through electron microscopy. Though multiple variants of negative-staining method have been introduced in the literature, the main principle lies at surrounding, permeating and embedding a thin layer of viral sample by dried amorphous or vitreous layer of heavy metal-containing cationic

or anionic salts. An electron micrograph of negatively stained sample is primarily generated by differential electron scattering due to the difference in thickness between viral sample and surrounding stain layer.[38] Some of the principle heavy metal salts that are employed on the biological samples are sodium/potassium phosphotungstate, uranyl acetate, sodium silicotungstate, and ammonium molybdate. The detailed procedure of negative staining is described in the following chart (Fig. 1).

Some of the limitations of negative staining include artefacts caused by drying, dehydration and flattening of biological specimens.[39] Theoretically, intra-molecular information, such as alpha helices or beta sheet structures of proteins, is very rare to be seen by negative staining. Hence, interpretation of micrographs of viruses becomes difficult if viruses possess complex or no symmetry. However, despite its multiple limitations, the negative-staining technique continues to be used widely within the fields of virology for many decades. Some of the negatively stained electron micrographs of bacteriophages are presented in Figs. 2 and 3.

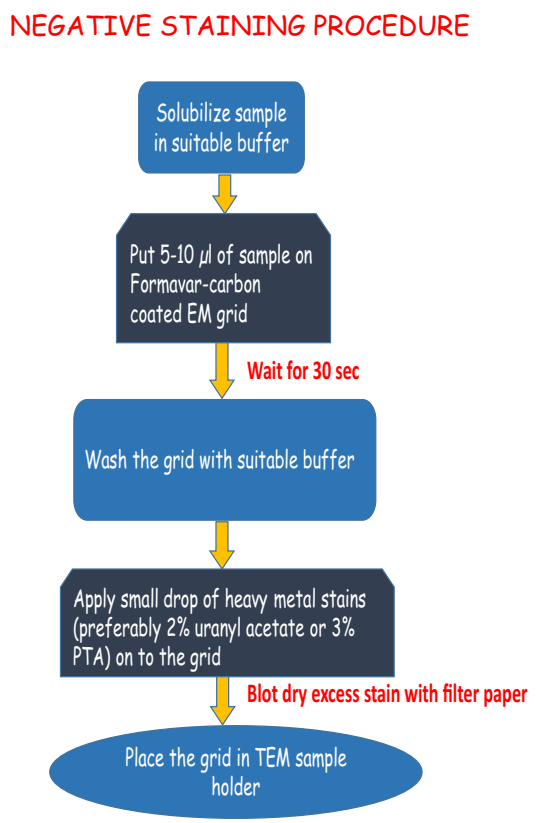

Figure 1: Illustration of negative-staining procedure on biological specimen.

The limitations of negative staining were overcome with the advent of cryoEM. The concept of cryoEM was realized in practice when Dubochet and McDowall were first able to vitrify water samples[40] and subsequently could vitrify biological samples.[8] As the specimens are frozen in its native state, it minimizes artefacts caused by drying of sample during negative staining. The main advantage of cryoEM over negative stain is the achievement of high-resolution structures. The excess electron scattering from the sample in comparison to surrounding buffer provides sufficient contrast to visualise specimens in absence of any stain. However, the best resolution that can be obtained using cryoEM depends on the specimen preparation methods and the technical superiority of the electron microscope. The sample in cryoEM must be frozen extremely rapidly at a rate of ~ 10^6 °C/s so that the water surrounding the specimen is fixed in a vitreous state.[41–43] If freezing occurs slowly, crystalline ice is formed. Ice contamination disturbs the structural integrity of the specimen. Formation of crystalline ice also

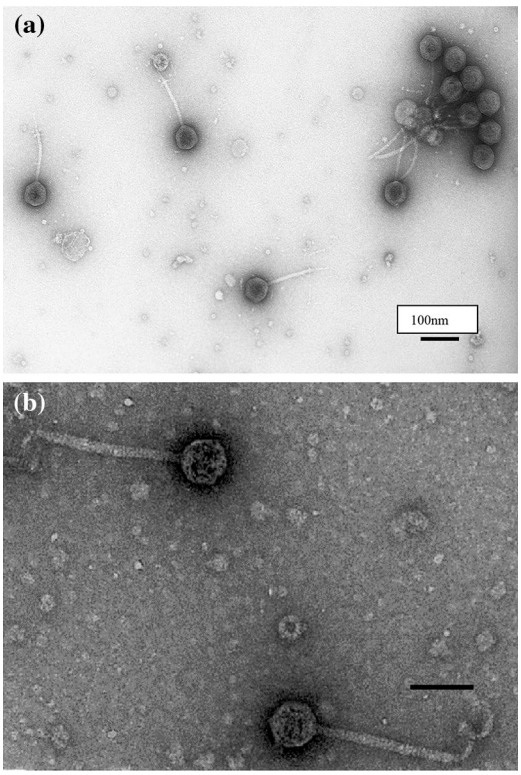

Figure 2: **a** Negatively stained group-IV bacteriophage of host *Vibrio cholerae* belonging to *Siphoviridae* family. **b** Negatively stained image of pseudomonas phage of *Siphoviridae* family. Bar = 100 nm.

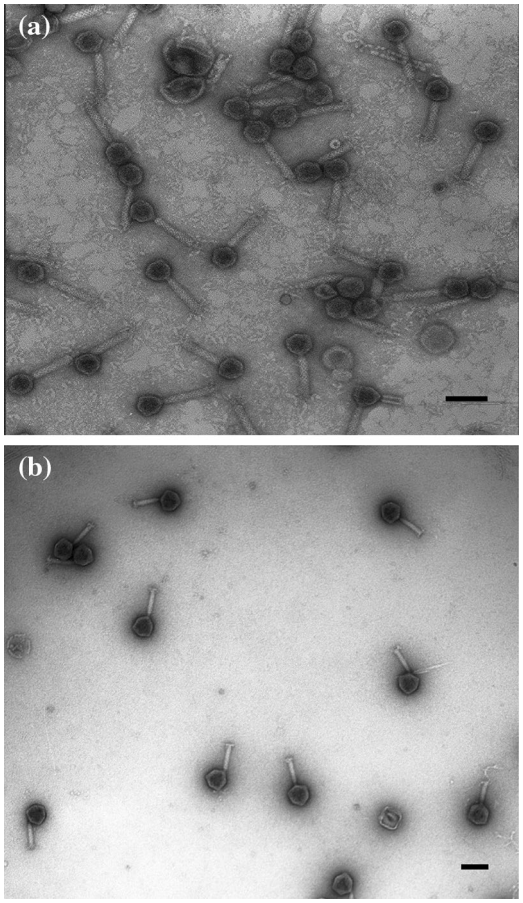

Figure 3: **a** Micrograph showing negatively stained D10 vibriophage belonging to *Myoviridae* family. Bar represents 100 nm. **b** Negatively stained vibriophage M4 of *Myoviridae* family. Bar represent 100 nm.

sacrifices the image quality as they diffract electrons. Contamination, such as hexagonal ice, can also occur during the freezing process. This can be avoided by working in humidity-controlled environments and minimising ice contamination in the liquid nitrogen. The process of sample preparation of cryo is described in Fig. 4.

Viruses are naturally occurring icosahedral assemblies with 532 point group symmetry. Some viruses have identical subunits while some possess more than one kind of subunits.[44] These icosahedral particles produce images containing more information per particle than other low-symmetric particles. As a result, a significant number of icosahedral particles have reached resolutions better than 10 Å and in future it will be possible to reconstruct three-dimensional structures of viruses in a regular manner with resolution better than of 3 Å from cryo-fixed 2-D images.[44] Some of the cryo-fixed bacteriophage samples are presented in the following images (Fig. 5a, b).

5 Bacteriophages and their Mesmerizing Structures

The viruses of bacteria, the bacteriophages, are very fascinating objects for structural biologists as they show immense diversity in their structure and genome. Bacteriophages survive in the harsh environment by infecting their host bacteria in two different manner; lytic or lysogenic. During lytic cycle, phages insert their DNA into their host organisms, phage DNA replicates inside and produces different phage proteins. After formation of complete phage particles, the host cell is lysed and releases phage particles. During lysogenic pathway, phage DNA gets enclosed inside host DNA and forms prophages. Prophages divide within the host cell (Fig. 6).

Typically, bacteriophages are non-enveloped viruses that are made up of a head which is connected to the tail through a protein complex called head-to-tail connector protein portal. The tail generally ends at an adsorption device called baseplate (Fig. 7). Inside the capsid, the genome is packed very tightly. Bacteriophages show differences in their capsid structure. While some phages have helical capsid like the filamentous phages, most phages have icosahedral capsid. Icosahedral assemblies generally have 532 point group symmetry and are made up of 60 identical or non-identical protein subunits.[44]

Bacteriophage tails are also very fascinating as they are evolved to receptor binding, penetration and delivery of genome into their host. Tailed phages are generally called *Caudovirales*.[45] Due to diversity in their tail morphology *Caudovirales* are classified into three families: *Siphoviridae* (having long non-contractile tails), *Myoviridae* (having long contractile tail) and *Podovoridae* (having short tail). Being contractile in nature *Myoviridae* phage tails have a contractile sheath enclosing the central tail tube.[46, 47] Upon initiation of infection, the sheath gets contracted, leaving the tube behind through which genome passes from the phage to the host cell.

The *Siphoviridae* and *Myoviridae* phages have a special adsorption device at the tip of their tail. This is commonly called baseplate and helps in host recognition and penetration of the host membrane for initiating infection process. Sometimes phages use protein receptors for binding with the host cells and possess conical tail tips like in phage SPP1,[48, 49] whereas some phages use polysaccharide receptor thus usually have broad

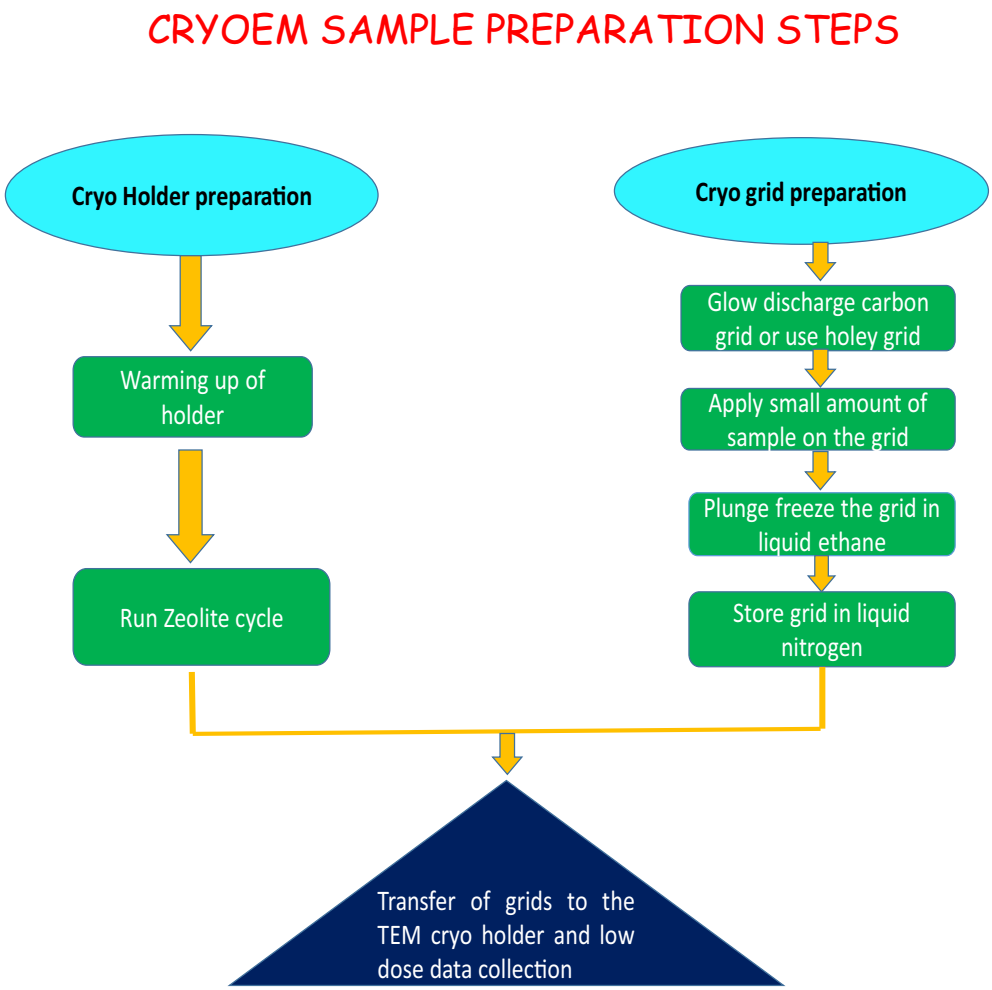

Figure 4: Steps of sample preparation for cryoEM.

and elaborate baseplate at the tail tip like in phage TP901-1.[47, 50, 51] Moreover, most phages have tail fibres or spikes attached at the bottom of the tail. Some phages have short tail fibres and some phages have long tail fibres. These tail fibres help the phage to anchor to the host cell membrane.

6 Three-Dimensional Structure of Bacteriophages Determined by Electron Microscopy and Image Reconstruction Techniques

Due to their highly symmetric structures, so far three-dimensional structure of many bacteriophages has been determined. It started with tail structures of T4 and continues with many other phages of different host group.

6.1 Coliphages

Let us start this account with smallest bacteriophage φX174. It is a ssDNA phage of host *E. coli*. Like other phages it also packages its single-stranded DNA inside the protein capsid. The DNA packaging intermediate's structure of this phage capsid was reconstructed by Leodevico et al. in 1995 following cryoEM and image reconstruction technique.[52] The icosahedral capsid has triangulation number $T=1$ arrangement of protein subunits.

Another most widely studied bacteriophage of host *E. coli* is T4. It is a large, ds DNA phage. It has a prolate head of size 1150 Å in length and 850 Å in width with hemi-icosahedral ends[53] which encapsidate the genomic DNA (Fig. 8). The head is attached with a 1000 Å long and 210 Å wide contractile tail [54–56] which ends at a 460 Å diameter baseplate.[57] The helical tail of T4 has an axial rise of 39.8 Å and turn angle of 21.4°. Long tail fibres of length 1450 Å are also seen to be attached to the baseplate.[58] The head, tail, and fibres are assembled in ordered pathways to form the complete virus particle.[59, 60]

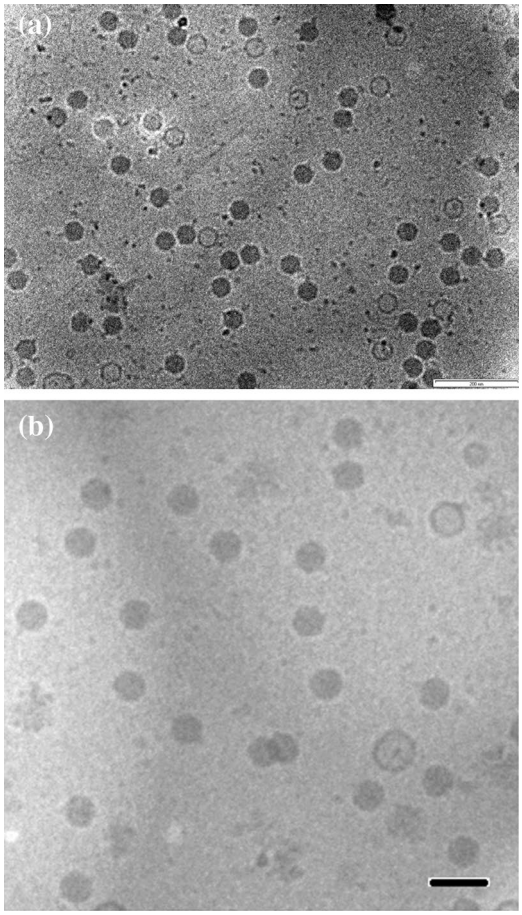

Figure 5: **a** Frozen-hydrated S20 vibriophage. The bar represents 200 nm. **b** Cryo-fixed image of vibriophage S5. Bar = 100 nm.

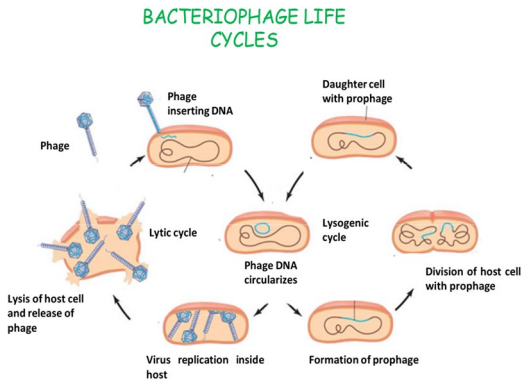

Figure 6: Schematic representation of bacteriophage life cycles.

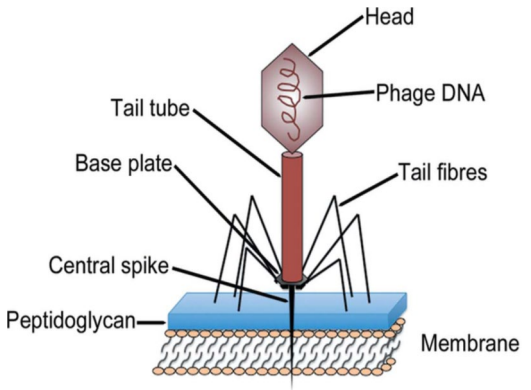

Figure 7: Schematic diagram of a bacteriophage taken with permission from *Viruses and viral proteins Nuria Verdaguer, Diego Ferreroa and Mathur, R. N. Murthy, (2014). IUCrJ 1, 492–504,* https://doi.org/10.1107/s205225251402003x.

Further, the structure of model phage Lambda of *E. coli* was also determined following cryoEM in 2008. Carragher et al. reported the icosahedral capsid structure of Lambda phage at 6.8 Å resolution at 0.5 FSC and also showed the localization of protein gp D in the capsid.[61]

Jiang et al. in 2014 displayed the atomic models of intermediate stages of another coliphage T7 during capsid maturation.[62] They have used cryoEM and single-particle reconstruction technique to get three-dimensional structure of procapsid at 4.6 Å resolution, an early stage DNA packaging intermediates at 3.5 Å, a later stage packaging intermediates at 6.6 Å and a final mature virus particle at 3.6 Å resolution. In 2013, Hu et al. used cryoET for showing extensive structural remodelling of T7 phage at nanometre range resolution during infection process.[63]

Baker et al. reported the structure of another phage CUS-3 that infects serotype K1 *E. coli*.[64] They were able to reconstruct this short-tailed dsDNA bacteriophage virion at 6.8 Å resolution following cryoEM and single-particle analysis technique.

An interesting phage system of host *E. coli* is P2–P4 bacteriophage system. P4 acts as a parasite of P2 phage and does not code for any structural gene.[65] Normally, P2 capsid is approx. 600 Å in diameter. However, the P4 capsid is only 450 Å in diameter. In 1992, Dokland et al. reported the structure of both P2 and P4 phage at a low resolution of 45 Å following cryoEM and image reconstruction technique.[66] P2 capsid has $T=7$ symmetry, whereas P4 has $T=4$ symmetry.

Another interesting phage of *E. coli* is PRD1. It is a tail-less icosahedral phage, containing an internal lipid membrane. It belongs to *Tectiviridae* family.[67] In 1995, Butcher et al. reconstructed the three-dimensional structure of phage PRD1 at 20 Å resolution. It has a $T=25$ lattice symmetry in its capsid. The structure of mutant virion at

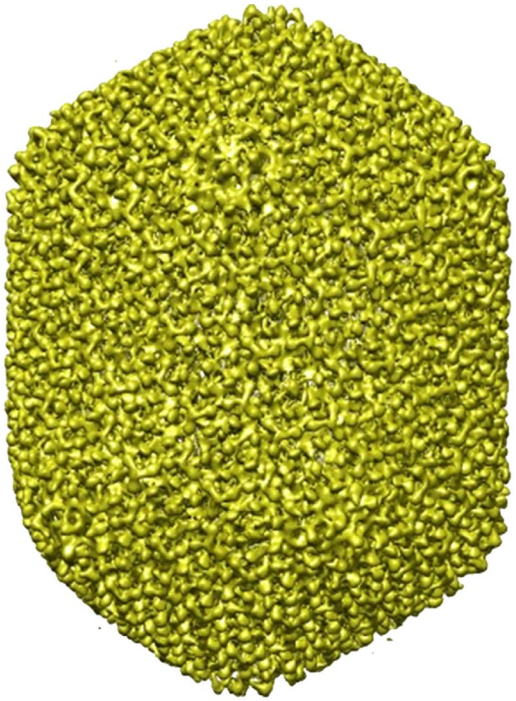

Figure 8: Three-dimensional structure of bacteriophage T4 capsid at 21Å resolution.[53] EMDB ID: 1414.

28 Å showed the interaction between outer capsid protein and inner lipid membrane.[68]

6.2 Pseudomonas Phage

Phi6 is one of the best studied bacteriophage of *Cystoviridae* family, which infects *Pseudomonas syringae* species. This dsRNA bacteriophage contains a capsid surrounded by a lipid envelope. In 1997 Butcher et al. reconstructed the neucleocapsid of the phage without the lipid envelop.[69] The reconstruction showed that the neucleocapsid possess $T=13$ lattice arrangement (Fig. 9).

6.3 Shigella Phage

Bacteriophage Sf6 infects the common human pathogen *Shigella flexneri*, and in the prophage state, Sf6 can affect the host pathogenecity.[70, 71] In the year 2012 Baker et al. processed and reconstructed the icosahedral capsid of Sf6 at a resolution of 7.8 Å.[72] The morphology of the Sf6 procapsid is quite similar to that of the P22 procapsid shell. SF6 capsid exhibits $T=7$ symmetry. The dsDNA is tightly packed inside the Sf6 capsid within a series of concentric shells (Fig. 10).[72] The Sf6 capsid undergoes expansions and forms a structure with highest diameter of 90 Å.

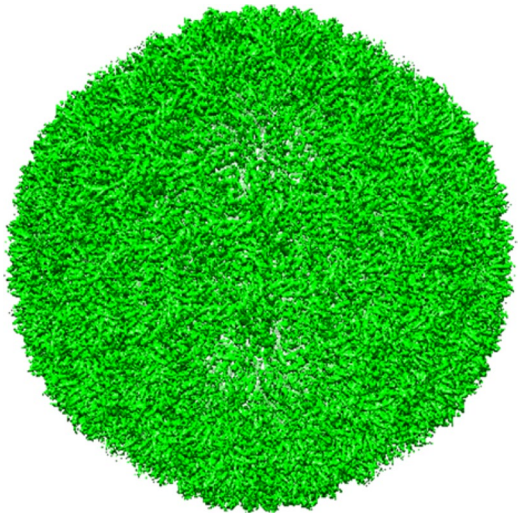

Figure 9: Reconstructed phi6 phage capsid at 4.1 Å resolution.[91] EMDB ID: 3571.

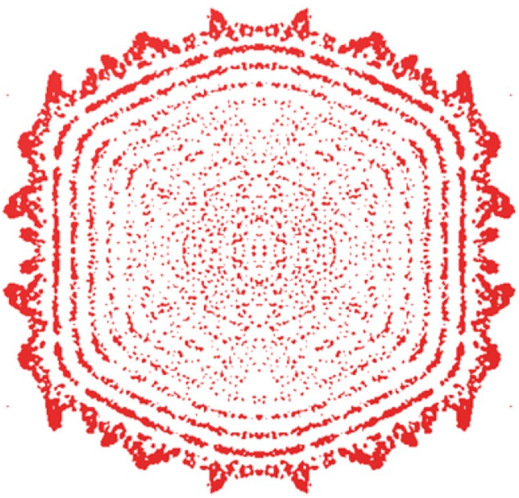

Figure 10: Section of Sf6 phage capsid showing packaging of DNA inside.[72] EMDB ID : 5728.

6.4 Salmonella Phage

Another remarkable work was done by Baker et al. on P22 bacteriophage.[73] P22 belongs to *Podoviridae* family and infects *Salmonella enterica* serovar *Typhimurium*. They asymmetrically reconstructed P22 virion at 7.8-Å resolution with imposed symmetry at 5.0-Å resolution in 2011. A modified capsid protein model nicely fits the reconstructed density.

6.5 Vibriophage

Like T4 of host *E. coli*, the structure of many bacteriophages of host *V. cholerae* has been solved till

date. In 2007, the capsid structure of two *Podoviridae* vibriophages S5[74] and S20[75] have been three-dimensionally reconstructed following cryoEM. The three-dimensional reconstructed structure of S20 phage in 2007 by Dutta et al. was the first reported cryoEM low-resolution structure from India.

In 2017, the complete structure of another vibriophage D10 belonging to *Myoviridae* family has been reported following electron microscopy and three-dimensional reconstruction technique.[76] Vibriophage D10 consists of 500Å wide icosahedral head with 850 Å long tail which ends at 250 Å wide baseplate. The contractile tail of D10 has an axial rise of 36.8 Å and turn angle of 24.0°.

6.6 Bordetella Phage

In, 2009 Dai et al. reported the three-dimensional structure of a bacteriophage BPP-1 of *Podoviridae* family, which infects *Bordetella* species.[77] Following cryoET analysis technique the authors managed to get a 7-Å resolution capsid structure of the phage. This phage can switch its specificity by mutating the major tropism-determinant protein MTD.[77] The location of this protein MTD was also determined following electron tomographic reconstruction of labelled BPP1 phage particles.

6.7 Bacillus Phage

Bacteriophage phi29 is one of smallest known tailed phages[78] which infect *Bacillus subtilis* and belongs to *Podoviridae* family. In 2006, Rossmann et al. determined the three-dimensional structure of this fibre-less isometric phage at 7.9 Å resolution by cryo-electron microscopy, which allows the identification of alpha helices and beta sheets present in the capsid protein.[79]

Further, White et al. have shown the capsid structure of another phage SPP1 of host *Bacillus subtilis* in 2012 by cryoEM and single-particle analysis method. They have determined the structures of capsid at different stages after viral genome packaging at sub-nanometre resolution.[80] They reported the structure of capsid which lacks gp12 protein (HΔ12) in the capsid at 15.1 Å resolution, structure of capsid with gp12 protein (H) at 11.7 Å, DNA-full phage capsid (FP) at 8.8 Å, and structure of empty phage capsid (EP) at 10.5 Å resolution.

6.8 Mycobacterium Phage

In 2013, the structure of first *Mycobacterium abscessus subsp. bolletii* phage Araucaria was reported by Bebeacua et al.[81] The mature capsid of phage Araucaria was reconstructed at low resolution of 30 Å. The capsid measures 600 Å in diameter and attaches with 160 Å wide tail which extends over 1100 Å between the connector and the baseplate. Belonging to Siphoviridae family, it has a non-contractile tail of axial rise 40.6 Å and turn angle 17.2°.

6.9 Staphylococcus Phage

The three-dimensional structure of a *Myoviridae* phage phi812 of host *Staphylococcus aureus* was reconstructed by Novácek et al.[82] They have reconstructed the capsid at 3.8 Å resolution with cryo-fixed micrographs. The capsid measures 900 Å in diameter and showed the residues of major capsid protein forming the folds. The contractile tail of phi812 measures 2020 Å in length and 278 Å in width having an axial rise of 18.8 Å and turn angle 30.7°.

6.10 Lactococcal Phage

Lactococcus lactis is a Gram-positive bacterium used for fermenting cheese and other dairy product. In 2013, the complete three-dimensional structure of Lactococcal phages TP901-1[83], P2[84] belonging to *Siphoviridae* family has also been reported following cryoEM and three-dimensional reconstruction technique. The capsid structure of TP901-1 and P2 was reconstructed at 15 Å resolution and 13 Å resolution, respectively. The mature capsid of phage TP901-1 has a diameter of 660 Å which attaches with the non-contractile tail of width 110 Å and length 1180 Å. The tail of the phage having an axial rise of 38 Å and turn angle 22.4° was reconstructed from negatively stained micrographs at 20 Å. P2 phage capsid measures 690 Å and has a non-contractile tail of length 1160 and 160 Å width with an axial rise of 37.4 Å and turn angle 46.3°. Both the structures have shown the arrangement of the genome inside the capsid.

6.11 Cyanophage

Following cryoET analysis technique, it was also possible to show the assembly of virus intermediates during host cell infection. In 2013, Chiu et al. have shown the fascinating structures of virus assembly intermediates of cyanophages during infection inside the marine cyanobacterium by cryoET.[85]

6.12 Bacteriophage MS2

Bacteriophage MS2 is a species of the Levivirus genus in the *Leviviridae* family of small, positive-sense, single-stranded ribonucleic acid (RNA)

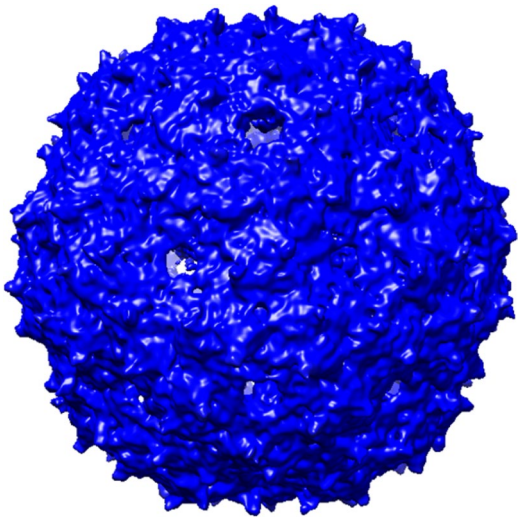

Figure 11: Bacteriophage MS2 capsid reconstructed at 10.2 Å.[87] EMDB ID: 3403.

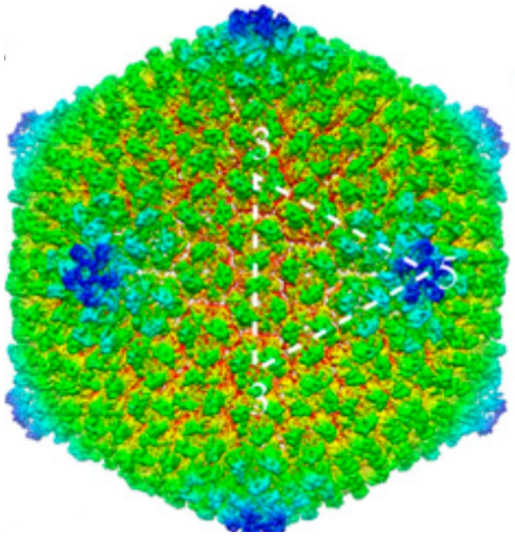

Figure 12: Reconstructed capsid of virophage "Sputnik" at 3.5 Å resolution. Reproduced with permission from *Structure of Sputnik, a virophage, at 3.5-Å resolution. Xinzheng Zhang, Siyang Sun, Ye Xiang, Jimson Wong, Thomas Klose, Didier Raoult, and Michael G. Rossmann, 2012, PNAS 109:45 18431–18436,* https://doi.org/10.1073/pnas.1211702109.

bacteriophages that infect their host via adsorption to bacterial pili.[86] The MS2 genome is one of the smallest known phage comprising just 3569 nucleotides. Asymmetric reconstruction of MS2 phage capsid by cryoET technique yields a structure at 4.1 Å resolution which reveals the genome structure inside of the capsid (Fig. 11).[87]

6.13 Virophage 'Sputnik'

Sputnik, virus of a giant virus Mamavirus, has many similarities with a bacteriophage. Thus, it is considered as a bacteriophage and was named as virophage.[88] The three-dimensional structure of the dsDNA virophage Sputnik was determined by Rossmann et al.[89] They have achieved a resolution of 3.5 Å of the density map of the icosahedral virus Sputnik processed through cryoEM. At this near-atomic resolution, the map is sufficient to verify the amino acids present in the capsid proteins and to identity the pentameric protein forming the five-fold vertices. The capsid is shown to be organized into $T=27$ (Fig. 12).

7 Conclusions

Bacteriophage has proven to be a model system for structural studies from the day when the first electron micrograph was taken with the electron microscope in 1940.[15] Since then it has proved to be useful also in the development of image processing methodologies. Incidentally, micrograph of the first frozen-hydrated unstained sample was also of a bacteriophage that had been taken in 1983.[8] After development of cryoEM in late 1980s, the resolution of electron micrographs has improved in a phenomenal way in nearly seven decades. Incidentally, over almost the same period deadly bacteria have started developing resistance to many antibiotics. There is thus a need for an alternate therapy like phage therapy. Bacteriophages specifically infect bacterial cells, therefore, offer variety of potential uses in the area of biomedicine. They easily undergo variety of surface modifications due to their high genetic flexibility that allow bacteriophages to be used for targeted delivery of therapeutic genes. Moreover, the safety profile of these viruses paves the way for their potential use as cancer gene therapy platforms.[90] Structural details of bacteriophages help to understand the inside molecular mechanisms during phage maturation. Bacteriophages interact with their host through host membrane receptors. Nowadays, the high-resolution structure of bacteriophages gives the idea of protein folding pattern upon initiation of infection. Also the near-atomic resolution structure of bacteriophage may prove to be useful in developing an artificial nano-container capable of dispensing drugs.

Received: 16 April 2018 Accepted: 21 June 2018
Published online: 11 July 2018

References

1. Adams MH (1959) Bacteriophages. Wiley (Interscience), New York
2. William CS (2012) The strange history of phage therapy. Bacteriophage 2(2):130–133. https://doi.org/10.4161/bact.20757
3. Daniel BG, Jonathan ES, Chad WE, Vincent AF (2013) Novel bacteriophage lysin with broad lytic activity protects against mixed infection by *Streptococcus pyogenes* and methicillin-resistant *Staphylococcus aureus*. Antimicrob Agents Chemother 57(6):2743–2750. https://doi.org/10.1128/aac.02526-12
4. Yen M, Carrins LS, Camilli A (2017) A cocktail of three virulent bacteriophages prevents Vibrio cholerae infection in animal models. Nat Commun 1(8):14187. https://doi.org/10.1038/ncomms14187
5. Chattopadhyay DJ, Sarkar BL, Ansari MQ, Chakrabarti BK, Roy MK, Ghosh AN, Pal SC (1993) New phage typing scheme for *Vibrio cholerae* O1 biotype El Tor strains. J Clin Microbiol 31:1579–1585
6. Taylor KA, Glaeser RM (1976) Electron microscopy of frozen, hydrated protein crystals. J Ultrastruct Res 55:448–456
7. Heide HG (1982) Design and operation of cold stages. Ultramicroscopy 10:125–154
8. McDowall AW, Chang JJ, Freeman R, Lepault J, Walter CA, Dubochet J (1983) Electron microscopy of frozen hydrated sections of vitreous ice and vitrified biological samples. J Microsc 131:1–9
9. DeRosier DJ, Klug A (1968) Reconstruction of three dimensional structures from electron micrographs. Nature 217:130–134. https://doi.org/10.1038/217130a
10. Roman IK, Josue GB, Inara A, Javier V, Andris K, Kaspars T, Jose C, Abraham JK (2016) Asymmetric cryo-EM reconstruction of phage MS2 reveals genome structure in situ. Nat Commun 7:12524
11. Chen Z, Sun L, Zhang Z, Fokine A, Sanchez VP, Hanein D, Jiang W, Rossmann MG, Rao VB (2017) Cryo-EM structure of the bacteriophage T4 isometric head at 3.3-Å resolution and its relevance to the assembly of icosahedral viruses. Proc Natl Acad Sci USA. 114(39):E8184–E8193. https://doi.org/10.1073/pnas
12. Rossmann MG (2013) Structure of viruses: a short history. Q Rev Biophys 46:133–180. https://doi.org/10.1017/s0033583513000012
13. Caspar DL (1956) Structure of bushy stunt virus. Nature 177:475–476
14. Klug A, Finch JT, Franklin RE (1957) Structure of turnip yellow mosaic virus. Nature 179:683–684. https://doi.org/10.1038/179683b0
15. Ruska H (1940) Visualization of bacteriophage lysis in the hypermicroscope. Naturwissenschaften 28:45–46
16. Hall CE (1966) Introduction to electron microscopy, 2nd edn. McGraw-Hill, New York
17. Brenner S, Horne RW (1959) A negative staining method for high resolution electron microscopy of viruses. Biochim Biophys Acta 34:103–110. https://doi.org/10.1016/0006-3002(59)90237-9
18. Crowther RA (1971) Procedures for three-dimensional reconstruction of spherical viruses by Fourier synthesis from electron micrographs. Philos Trans R Soc Lond B Biol 261:221–230. https://doi.org/10.1098/rstb.1971.0054
19. Rosenthal PB (2015) High symmetry to high resolution in biological electron microscopy: a commentary on Crowther (1971) 'Procedures for three-dimensional reconstruction of spherical viruses by Fourier synthesis from electron micrographs'. Philos Trans R Soc Lond B Biol Sci 370:1666. https://doi.org/10.1098/rstb.2014.0345
20. Battisti AJ, Meng G, Winkler DC, Mcginnes LW, Plevka P, Steven AC, Morrison TG, Rossmann MG (2012) Structure and assembly of a paramyxovirus matrix protein. Proc Natl Acad Sci USA 109:13996–14000
21. Rossmann MG, Battisti AJ, Plevka P (2011) Future prospects, recent advances in electron cryomicroscopy. In: Ludtke SJ, Prasad BVV (eds) Advances in protein chemistry and structural biology, vol 82. Part B. Academic Press, San Diego, pp 101–121
22. Harrison SC (2010) Virology. Looking inside adenovirus. Science 329:1026–1027
23. Liu H, Jin L, Koh SB, Atanasov I, Schein S, Wu L, Zhou ZH (2010) Atomic structure of human adenovirus by cryoEM reveals interactions among protein networks. Science 329:1038–1043
24. Reddy VS, Natchiar SK, Stewart PL, Nemerow GR (2010) Crystal structure of human adenovirus at 3.5 Å resolution. Science 329:1071–1075
25. Abad-Zapatero C, Abdel-Meguid SS, Johnson JE, Leslie AG, Rayment I, Rossmann MG, Suck D, Tsukihara T (1980) Structure of southern bean mosaic virus at 2.8 Å resolution. Nature 286:33–39
26. Harrison SC, Olson AJ, Schutt CE, Winkler FK, Bricogne G (1978) Tomato bushy stunt virus at 2.9 Å resolution. Nature 276:368–373
27. Jiang W, Tang L (2017) Atomic cryoEM structures of viruses. Curr Opin Struct Biol 46:122–129. https://doi.org/10.1016/j.sbi.2017.07.002
28. Chiu W, Baker ML, Jiang W, Dougherty M, Schmid MF (2005) Electron cryomicroscopy of biological machines at subnanometer resolution. Structure 13:363–372
29. Baker ML, Zhang J, Ludtke SJ, Chiu W (2010) CryoEM of macromolecular assemblies at near-atomic resolution. Nat Protoc 5:1697–1708
30. Hryc CF, Chen DH, Chiu W (2012) Near-atomic-resolution CryoEM for molecular virology. Curr Opin Virol 1(2):110–117. https://doi.org/10.1016/j.coviro.2011.05.019
31. Suloway C, Pulokas J, Fellmann D, Cheng A, Guerra F, Quispe J, Stagg S, Potter CS, Carragher B (2005)

Automated molecular microscopy: the new Leginon system. J Struct Biol 151:41–60
32. Henderson R, Glaeser RM (1985) Quantitative analysis of image contrast in electron micrographs of beam sensitive crystals. Ultramicroscopy 16:139–150
33. Kuhlbrandt W (2014) The resolution revolution. Science 343:1443–1444
34. Nogales E (2015) Scheres SH (2015) Cryo-EM: a unique tool for the visualization of macromolecular complexity. Mol Cell 58(4):677–689. https://doi.org/10.1016/j.molcel.2015.02.019
35. Brilot AF, Chen JZ, Cheng A, Pan J, Harrison SC, Potter CS, Carragher B, Henderson R, Grigorieff N (2012) Beam-induced motion of vitrified specimen on holey carbon film. J Struct Biol 177:630–637
36. Campbell MG, Cheng A, Brilot AF, Moeller A, Lyumkis D, Veesler D, Pan J, Harrison SC, Potter CS, Carragher B, Grigorieff N (2012) Movies of ice-embedded particles enhance resolution in electron cryomicroscopy. Structure 20:1823–1828
37. Xueming L, Paul M, Shawn Z, Christopher RB, Michael BB, Sander G, David AA, Yifan C (2013) Electron counting and beam-induced motion correction enable near-atomic-resolution single-particle cryo-EM. Nat Methods 10:584–590. https://doi.org/10.1038/nmeth.2472
38. Hayat MA, Miller SE (1990) Negative staining. In: Hayat MA, Miller SE (eds) Negative staining. McGraw-Hill Publishing Company, New York, pp 36–48
39. Carlo SD, Harris JR (2011) Negative staining and Cryo-negative staining of Macromolecules and Viruses for TEM. Micron 42(2):117–131. https://doi.org/10.1016/j.micron.2010.06.003
40. Dubochet J, McOowall AW (1981) Vitrification of pure water for electron microscopy. J Microsc 124:KP3–RP4
41. Thompson RF, Walker MC, Siebert A, Stephen PM, Neil AR (2016) An introduction to sample preparation and imaging by cryo-electron microscopy for structural biology. Methods 100:3–15. https://doi.org/10.1016/j.ymeth.2016.02.017
42. Baker LA, Rubinstein JL (2010) Radiation damage in electron cryomicroscopy. Methods Enzymol 481:371–388
43. Dubochet J, Adrian M, Chang JJ, Homo JC, Lepault J, McDowall AW (1988) Cryo-electron microscopy of vitrified specimens. Q Rev Biophys 21:129–228. https://doi.org/10.1017/s0033583500004297
44. Henderson R (2004) Realizing the potential of electron cryo-microscopy. Q Rev Biophys 37(1):3–13. https://doi.org/10.1017/s0033583504003920
45. Ackermann HW, Furniss AL, Kasatiya SS, Lee JV, Mbiquino A, Newman FS, Takeya K, Viev JF (1983) Morphology of Vibrio cholerae typing phages. Ann Virol 134E:387–404
46. Leiman PG, Shneider MM (2012) Contractile tail machines of bacteriophages. Adv Exp Med Biol 726:93–114. https://doi.org/10.1007/978-1-4614-0980-9_5
47. Leiman PG, Arisaka F, Raaij MJ, Kostyuchenko VA, Aksyuk AA, Kanamaru S, Rossmann MG (2010) Morphogenesis of T4 tail and tail fibers. Virol J 3(7):355. https://doi.org/10.1186/1743-422x-7-355
48. Plisson C, White HE, Auzat I, Zafarani A, Sao-Jose C, Lhuillier S, Tavares P, Orlova EV (2007) Structure of bacteriophage SPP1 tail reveals trigger for DNA ejection. EMBO J 26(15):3720–3728
49. Pell LG, Kanelis V, Donaldson LW, Howell PL, Davidson AR (2009) The phage lambda major tail protein structure reveals a common evolution for long-tailed phages and the type VI bacterial secretion system. Proc Natl Acad Sci USA 106(11):4160–4165
50. Veesler D, Spinelli S, Mahony J, Lichiere J, Blangy S, Bricogne G, Legrand P, Ortiz-Lombardia M, Campanacci V, Sinderen D, Cambillau C (2012) Structure of the phage TP901-1 1.8 MDa baseplate suggests an alternative host adhesion mechanism. Proc Natl Acad Sci USA 109(23):8954–8958. https://doi.org/10.1073/pnas.1200966109
51. Sciara G, Bebeacua C, Bron P, Tremblay D, Ortiz-Lombardia M, Lichiere J, Heel MV, Campanacci V, Moineau S, Cambillau C (2010) Structure of lactococcal phage p2 baseplate and its mechanism of activation. Proc Natl Acad Sci USA 107(15):6852–6857
52. Leodevico LI, Terje HOD, Cynthia LM, Holland CR, Zorina B, Robert M, Rossmann MG, Baker TS, Nino LI (1995) DNA packaging intermediates of bacteriophage φX174. Structure 4:353–363. https://doi.org/10.1016/s0969-2126(01)00167-8
53. Fokine A, Chipman PR, Leiman PG, Mesyanzhinov VV, Rao VB, Rossmann MG (2004) Molecular architecture of the prolate head of bacteriophage T4. Proc Natl Acad Sci USA 101:6003–6008
54. Aksyuk AA, Leiman PG, Kurochkina LP, Schneider MM, Kostyuchenko V, Mesyanzhinov VV, Rossmann MG (2009) The tail sheath structure of bacteriophage T4: a molecular machine for infecting bacteria. EMBO J 28:821–829
55. Aksyuk AA, Kurochkina LP, Fokine A, Forouhar F, Mesyanzhinov VV, Tong L, Rossmann MG (2011) Structural conservation of the Myoviridae phage tail sheath protein fold. Structure 19:1885–1894
56. Kostyuchenko VA, Chipman PR, Leiman PG, Arisaka F, Mesyanzhinov VV, Rossmann MG (2005) The tail structure of bacteriophage T4 and its mechanism of contraction. Nat Struct Mol Biol 12:810–813
57. Kostyuchenko VA, Leiman PG, Chipman PR, Kanamaru S, Van MJ, Arisaka F, Mesyanzhinov VV, Rossmann MG (2003) Three-dimensional structure of bacteriophage T4 baseplate. Nat Struct Biol 10:688–693
58. Aksyuk AA, Leiman PG, Shneider MM, Mesyanzhinov VV, Rossmann MG (2009) The structure of gene product 6 of bacteriophage T4, the hinge-pin of the baseplate. Structure 17:800–808

59. Berget PB, King J (1978) Isolation and characterization of precursors in T4 baseplate assembly. The complex of gene 10 and gene 11 products. J Mol Biol 124:469–486
60. Coombs DF, Arisaka F (1994) T4 tail structure and function. In: Karam JD (ed) Molecular Biology of Bacteriophage T4. American Society for Microbiology, Washington, D.C., pp 259–281
61. Lander GC, Evilevitch A, Jeembaeva M, Potter CS, Carragher B, Johnson JE (2008) Bacteriophage lambda stabilization by auxiliary protein gpD: timing, location, mechanism of attachment determined by cryoEM. Structure 9:1399–1406. https://doi.org/10.1016/j.str.2008.05.016
62. Guoa F, Liua Z, Fanga P, Zhang Q, Wright ET, Wu W, Zhang C, Vago F, Rena Y, Jakana J, Chiu W, Serwer P, Jiang W (2014) Capsid expansion mechanism of bacteriophage T7 revealed by multistate atomic models derived from cryo-EM reconstructions. PNAS 111:E4606–E4614. https://doi.org/10.1073/pnas.1407020111
63. Hu B, Margolin W, Molineux IJ, Liu J (2013) The bacteriophage T7 virion undergoes extensive structural remodeling during infection. Science. https://doi.org/10.1126/science.1231887
64. Parent KN, Tang J, Cardone G, Gilcrease EB, Janssen ME, Olson NH, Casjens SR, Baker TS (2014) Three-dimensional reconstructions of the bacteriophage CUS-3 virion reveal a conserved coat protein I-domain but a distinct tailspike receptor-binding domain. Virology 464–465:55–66. https://doi.org/10.1016/j.virol.2014.06.017
65. Baker TS, Olson NH, Fuller SD (1999) Adding the third dimension to virus life cycles: three-dimensional reconstruction of Icosahedral viruses from cryo-electron micrographs. Microbiol Mol Biol Rev 63(4):862–922
66. Dokland T, Lindqvist BH, Fuller SD (1992) Image reconstruction from cryo-electron micrographs reveals the morphopoietic mechanism in the P2–P4 bacteriophage system. EMBO J 11(3):839–846
67. Butcher SJ, Manole V, Karhu NJ (2012) Lipid-containing viruses: bacteriophage PRD1 assembly. Adv Exp Med Biol 726:365–377. https://doi.org/10.1007/978-1-4614-0980-9_16
68. Butcher SJ, Bamford DH, Fuller SD (1995) DNA packaging orders the membrane of bacteriophage PRD1. EMBO J 14(24):6078–6086
69. Butcher SJ, Dokland T, Ojala PM, Bamford DH, Fuller SD (1997) Intermediates in the assembly pathway of the double-stranded RNA virus φ6. EMBO J 16(14):4477–4487
70. Clark CA, Beltrame J, Manning PA (1991) The oac gene encoding a lipopolysaccharide O-antigen acetylase maps adjacent to the integrase-encoding gene on the genome of *Shigella flexneri* bacteriophage Sf6. Gene 107(1):43
71. Verma NK, Brandt JM, Verma DJ, Lindberg AA (1991) Molecular characterization of the O-acetyl transferase gene of converting bacteriophage SF6 that adds group antigen 6 to *Shigella flexneri*. Mol Microbiol 1:71–75
72. Parent KN, Gilcrease EB, Casjens SR, Baker TS (2012) Structural evolution of the P22-like phages: comparison of Sf6 and P22 procapsid and virion architectures. Virology 427(2):177–188. https://doi.org/10.1016/j.virol.2012.01.040
73. Tang J, Lander GC, Olia AS, Li R, Casjens S, Prevelige PJ, Cingolani G, Baker TS, Johnson JE (2011) Peering down the barrel of a bacteriophage portal: the genome packaging and release valve in p22. Structure 19(4):496–502. https://doi.org/10.1016/j.str.2011.02.010
74. Mitra K, Ghosh AN (2007) Characterization of Vibrio cholerae O1 ElTor typing phage S5. Arch Virol. https://doi.org/10.1007/s00705-007-1021-2
75. Dutta M, Ghosh AN (2007) Physicochemical Characterization of El Tor Vibriophage S20. Intervirology 50:264–272. https://doi.org/10.1159/000102469
76. Sen A, Ghosh AN (2017) Visualizing a Vibrio cholerae O1 El Tor typing bacteriophage belonging to the Myoviridae group and the packaging of its genomic ends inside the phage capsid. J Biomol Struct Dyn 1:1–14. https://doi.org/10.1080/07391102.2017.1368416
77. Dai W, Hodes A, Hui WH, Gingery M, Miller JF, Zhou ZH (2010) Three-dimensional structure of tropism-switching Bordetella bacteriophage. PNAS 107(9):4347–4352. https://doi.org/10.1073/pnas.0915008107
78. Rajagopal BS, Reilly BE, Anderson DL (1993) Bacillus subtilis mutants defective in bacteriophage phi 29 head assembly. J Bacteriol 175(8):2357–2362
79. Xiang Y, Morais MC, Battisti AJ, Grimes S, Jardine PJ, Anderson DL, Rossmann MG (2006) Structural changes of bacteriophage 29 upon DNA packaging and release. EMBO J 25:5229–5239
80. White HE, Sherman MB, Brasilès S, Jacquet E, Seavers P, Tavares P, Orlova EV (2012) Capsid structure and its stability at the late stages of bacteriophage SPP1 assembly. J Virol 86(12):6768–6777. https://doi.org/10.1128/JVI.00412-12
81. Sassi M, Bebeacua C, Drancourt M, Cambillaua C (2013) The first structure of a mycobacteriophage, the *Mycobacterium abscessus* subsp. *bolletii* Phage Araucaria. J Virol 87(14):8099–8109
82. Novácek J, Siborová M, Benešík M, Pant R, Doškar J, Plevka P (2016) Structure and genome release of Twort-like Myoviridae phage with a double-layered baseplate. PNAS 113(33):9351–9356. https://doi.org/10.1073/pnas.1605883113
83. Bebeacua C, Lai L, Vegge CS, Brøndsted L, Heel MV, Veesler D, Cambillauc C (2013) Visualizing a complete *Siphoviridae* member by single-particle electron microscopy: the structure of Lactococcal Phage TP901-1. J Virol 87:1061–1068
84. Bebeacua C, Tremblay D, Farenc C, Chartier MC, Sadovskaya I, Heel MV, Veesler D, Moineau S, Cambillaua C (2013) Structure, adsorption to host, and infection mechanism of virulent Lactococcal Phage p2. J Virol 87(22):12302–12312

85. Dai W, Fu C, Raytcheva D, Flanagan J, Khant HA, Liu X, Rochat RH, Pettinge CH, Piret J, Ludtke SJ, Nagayama K, Schmid MF, King JA, Chiu W (2013) Visualizing virus assembly intermediates inside marine cyanobacteria. Nature. https://doi.org/10.1038/nature12604
86. Davis JE, Strauss JH, Sinsheimer R (1961) Bacteriophage MS2: another RNA Phage. Science 134:1427
87. Koning RI, Blanco JG, Akopjana I, Vargas J, Kazaks A, Tars K, Carazo JS, Koster AJ (2016) Asymmetric cryo-EM reconstruction of phage MS2 reveals genome structure in situ. Nat Commun 26(7):12524. https://doi.org/10.1038/ncomms12524
88. Raoult D (2015) How the virophage compels the need to readdress the classification of microbes. Virology 477:119–124
89. Zhang X, Sun S, Xiang Y, Wong J, Klose T, Raoult D, Rossmann MG (2012) Structure of Sputnik, a virophage, at 3.5-Å resolution. PNAS 109(45):18431–18436. https://doi.org/10.1073/pnas.1211702109
90. Bakhshinejad B, Karimi M, Sadeghizadeh M (2014) Bacteriophages and medical oncology: targeted gene therapy of cancer. Med Oncol 31(8):110. https://doi.org/10.1007/s12032-014-0110-9
91. Sun Z, Omari K, Kotecha A, Stuart DI, Poranen M, Huiskonen J (2017) Double-stranded RNA virus outer shell assembly by bona fide domain-swapping. Nat Commun 8:14814. https://doi.org/10.1038/ncomms14814

Sayani Das Did masters in Biotechnology from Jadavpur University, Kolkata and is CSIR-Senior Research Fellow at Electron microscopy division of National Institute of Cholera and Enteric Diseases, Kolkata. Her interest includes cryo-electron microscopy and 3-D image reconstruction of bacteriophages.

Amar Nath Ghosh is Emeritus Scientist at ICMR-National Institute of Cholera & Enteric Diseases, Kolkata. He retired from the same institute as a Director Grade Scientist and Head, Division of electron microscopy. His interest includes cryoelectron microscopy, tomography, 3-D structure and DNA electron microscopy of bacteriophages.